Scientific Validation of the Traditional Anti-Inflammatory Use of the Sapindus mukorossi Seed Kernel: In Vitro and In Silico Insights

Esther Lathazuali
Mizoram University
Hmingremhlua Sailo
Pachhunga University College
Martin Lalnunthara
Mizoram University
No given name Lalremliani
Mizoram University
No given name Lalawmpuia
Mizoram University
Laldinfeli Ralte
Mizoram University
Lalfakzuala Ralte
lalfaka@yahoo.com
Mizoram University

Research Article

Keywords: Sapindus mukorossi, Anti-inflammatory activity, Haemorrhoids, Molecular docking and dynamics, Ethnopharmacology

Posted Date: January 28th, 2026

DOI: https://doi.org/10.21203/rs.3.rs-8101955/v1

Additional Declarations: No competing interests reported.

Scientific Validation of the Traditional Anti-Inflammatory Use of the *Sapindus mukorossi* Seed Kernel: In Vitro and In Silico Insights

Esther Lathazuali[1], Hmingremhlua Sailo[2], Martin Lalnunthara[1], Lalremliani[1], Lalawmpuia[1], Laldinfeli Ralte[1] Lalfakzuala Ralte[1]*

* [1]*Department of Botany, Mizoram University, Aizawl-796004, Mizoram India*
* [2]*Department of Botany, Pachhunga University College, Aizawl-796001, Mizoram India*

Correspondence should be addressed to Lalfakzuala Ralte; lalfaka@yahoo.com

Abstract

S. mukorossi., commonly known as soapnut, is a traditional medicinal plant widely used in Asian ethnomedicine for treating infections and inflammatory disorders. However, systematic validation of its pharmacological potential remains limited. The antimicrobial and anti-inflammatory properties of *S. mukorossi* extract were evaluated using in vitro and biochemical assays. Cytotoxicity was assessed in RAW 264.7 macrophages using the MTT assay. Antibacterial activity was determined by agar well diffusion and minimum inhibitory concentration (MIC) assays against *Escherichia coli, Klebsiella pneumoniae*, and *Staphylococcus aureus*, while antifungal efficacy was tested against *Candida albicans* using disc diffusion. Anti-inflammatory potential was examined by measuring TNF-α levels through ELISA and cyclooxygenase-2 (COX-2) inhibition via a colorimetric assay. Molecular docking and molecular dynamics simulations, along with gmx_MMPBSA free energy calculations, were performed to assess the binding affinity of identified compounds (isosilybin A, orientin) with IRAK4. The extract demonstrated significant antimicrobial activity, producing notable inhibition zones against both Gram-positive and Gram-negative bacteria, with low MIC values indicating potent bacteriostatic effects. Antifungal activity against *C. albicans* was comparable to amphotericin B. The extract exhibited low cytotoxicity toward RAW 264.7 cells and effectively suppressed inflammatory mediators, showing dose-dependent inhibition of COX-2 activity and a marked reduction in TNF-α secretion. In silico analyses revealed stable binding of isosilybin A and orientin to IRAK4, as confirmed by molecular dynamics and gmx_MMPBSA free energy calculations (ΔGbind up to –47.8 kcal/mol). The findings substantiate the traditional use of *S. mukorossi* as a natural antimicrobial and anti-inflammatory agent. Its bioactive constituents may serve as potential leads for developing plant-derived therapeutic agents targeting infectious and inflammatory diseases. Further phytochemical characterization and molecular mechanism studies are warranted to elucidate the active principles and their targets.

Keywords: *Sapindus mukorossi*, Anti-inflammatory activity, Haemorrhoids, Molecular docking and dynamics, Ethnopharmacology

Introduction

Since time immemorial, plants have provided a wide range of benefits to humanity. In terms of nutrition, fruits and nuts play a vital role in the human diet, providing essential nutrients necessary for growth and development. Edible seeds and nuts are especially valued for their rich content of bioactive compounds, essential fatty acids, vitamins, amino acids, and minerals [1]. Traditional knowledge worldwide has relied on plant-based remedies to treat a variety of ailments, including skin diseases, gastrointestinal disorders, and inflammatory conditions. Indigenous communities have long recognized the therapeutic potential of wild edible plants [2]. In recent years, modern scientific interest in medicinal plants has revealed that their healing properties are due mainly to a diverse range of bioactive phytochemicals. Currently, understanding the chemical composition of these plants not only validates many traditional practices but also opens new avenues for integrating plant-based compounds into modern healthcare strategies [3].

Recently, researchers have also become more interested in applying current pharmacological, bioanalytical, and computational methods to determine if these traditional practices remain valid [4]. Phytochemical compounds from medicinal plants are also gaining recognition for their potential as safe, effective, and inexpensive alternatives to conventional drugs. Although pharmaceutical research is advancing rapidly, ethnomedicine remains a vital component of primary healthcare worldwide, particularly in resource-constrained areas [5]. Therefore, the use of evidence-based methods to record and evaluate traditional knowledge can help bring tried-and-true treatments into modern therapeutic models [6].

One such promising plant is *S. mukorossi* Gaertn., also known as "soapnut" or "reetha", a well-known medicinal plant that has been utilized for a long time in Ayurvedic and traditional healing practices. The pericarp of the fruit contains a high concentration of saponins, which are employed in plant medicines to treat skin conditions such as eczema, psoriasis, and dandruff [5]. Researchers studying phytochemistry have identified various medicinal components of the plant, including flavonoids, phenolic acids, and triterpenoidal saponins [7]. In addition to being used on the skin, seeds and seed oil have been reported to have anti-inflammatory, antibacterial, hepatoprotective, and spermicidal properties [8]. New research also indicates that *S. mukorossi* seed oil promotes the growth of fibroblasts and enhances wound healing [9]. It also lowers the production of nitric oxide in macrophages and possesses strong antioxidant properties because of the presence of compounds such as β-sitosterol, oleanane-type saponins, and α-tocopherol [10].

Folk medicine practitioners in the northeastern parts of India, such as in Mizoram, reported that eating *S. mukorossi* seeds alleviates symptoms of hemorrhoids. Local healers and elders also suggest eating the inner seed kernel for anal pain, swelling, and bleeding, especially in rural areas where regular treatments are difficult. There is anecdotal evidence that this practice is beneficial for therapy, but its effectiveness has not been scientifically proven. Although plants have a wide range of pharmacological effects, scientific evidence is still lacking concerning how they can be used to treat pain caused specifically by hemorrhoids, which are widely used [11]. Previous studies have demonstrated that *S. mukorossi* contains a diverse array of bioactive compounds, including oleanane and dammarane-type triterpenoidal saponins, flavonoids, phenolics, and essential fatty acids. Many of these compounds are known to have anti-inflammatory effects [12]. Although *S. mukorossi* has been used for a long time to treat inflammation, there is not much scientific evidence supporting its use for treating hemorrhoids.

This study therefore examines the anti-inflammatory properties of *S. mukorossi* seed kernel products against hemorrhoids by using both in silico and in vitro methods to bridge the gap between traditional knowledge and scientific evidence. In this study, metabolomics-based techniques (UHPLC-MS/MS) were employed to extract the active parts of seed extracts. This study also employs computer-aided methods, such as network pharmacology, molecular docking, and molecular dynamics (MD) models, to identify the most significant interactions between phytochemicals and targets and predict their binding affinity and complex stability. Several targeted in vitro assays have been used to confirm these computer estimates further.

Methodology

Sample collection:

Seeds, flowers, and leaves of *S. mukorossi* were collected from Aizawl, Mizoram (23.757786° N, 92.735737° E) (Fig. 1). It was identified and authenticated by Dr. Khomdram Sandhyarani Devi (Indian botanist and taxonomist), Associate Professor from the Department of Botany, Mizoram University with Accession No. MZUH001299.

S. mukorossi has long been used by the Sinner's Friend Camping Centre for treating hemorrhoids, underscoring its ethnomedicinal relevance. The kernels of the seeds were extracted via a Soxhlet apparatus with methanol as the solvent.

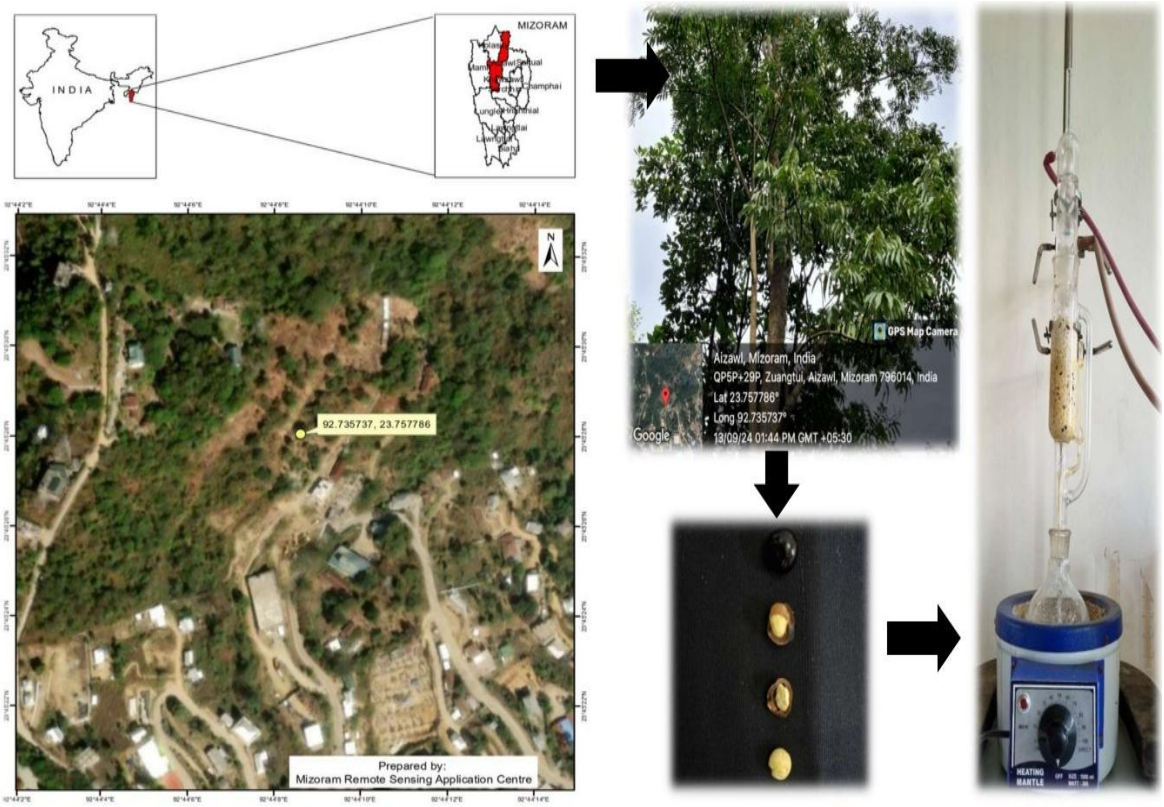

Fig. 1 Map and workflow for plant sample collection and extraction: (a) Sampling site location in Aizawl, Mizoram, India (geographic coordinates: 23.757786°N, 92.735737°E) visualized using satellite imagery; (b) Collection of plant material from the identified GPS site; (c) Seeds of the sampled plant species; (d) Subsequent extraction process using Soxhlet apparatus for chemical analysis.

LC–MS:

LC–ESI–MS² analysis of the *S. mukorossi* seed kernel extract was conducted using a Waters Alliance e2695 HPLC system coupled with a TQD mass spectrometer (Waters Corp., Milford, MA, USA). Separation was performed on an ACCUCORE C18 column (150 × 2.1 mm, 2.6 µm) with methanol containing 0.1% formic acid at 1.0 mL min^{-1} under gradient elution. Spectra were acquired in positive and negative ionization modes over m/z 150–2000 [13]. Data were processed using MassLynx™ software, and compounds were identified through database and literature comparison. Molecules meeting Lipinski's Rule of Five and favourable ADMET profiles were selected for *in silico* analysis.

Cytotoxicity Assay:

The cytotoxicity of seed kernel extracts of *S. mukorossi* was evaluated using the MTT assay. Cells (1×10^4 cells/well) were seeded in 96-well plates and cultured for 24 h in DMEM (HiMedia, AT149-1L) supplemented with 10% FBS (HiMedia, RM10432) and 1% penicillin–streptomycin (Sigma-Aldrich, P0781) at 37 °C in 5% CO_2. Cells were then treated with varying concentrations of the extract prepared in DMSO and diluted in serum-free medium. After 24 h, MTT solution (5 mg mL^{-1}) was added and incubated for 2 h. The supernatant was removed, formazan crystals were dissolved in 100 µL DMSO, and absorbance was measured at 540 nm using an ELISA plate reader (iMark™, Bio-Rad).

$$\text{Calculation: \% viable cells} = \frac{A_{Test}}{A_{Control}} \text{x}100$$

where A_{Test} = absorbance of the test sample and $A_{Control}$ = absorbance of the control.

Antimicrobial Assay

The extract was evaluated for its antifungal and antibacterial activities using standardized diffusion assays as described below.

Agar disc diffusion assay (antifungal activity)

Antifungal activity was determined using the disc diffusion method (Kirby-Bauer method) on Sabouraud Dextrose Agar (SDA) plates seeded with *C. albicans* (0.5 McFarland standard; ~1.5×10^8 CFU/mL). Sterile discs were impregnated with 10 µL of the extract at concentrations ranging from 0–100 mg/mL and placed on the inoculated agar surface. Amphotericin B (100 µg/disc) served as the positive control, while discs loaded with solvent alone acted as the negative control. Plates were incubated, and the zones of inhibition were measured to determine antifungal efficacy.

Agar well diffusion assay (antibacterial activity)

Antibacterial activity was assessed using the agar well diffusion method. Mueller–Hinton agar plates were inoculated with bacterial cultures adjusted to 0.5 McFarland standard (~1.5×10^8 CFU/mL). Wells were filled with different concentrations of the extract, and tetracycline and chloramphenicol served as positive controls. Solvent-only wells were used as negative controls. Plates were incubated at 37°C for 24 h, and the diameters of inhibition zones were recorded in millimeters.

Minimum inhibitory concentration (MIC) assay

The minimum inhibitory concentration (MIC) was determined using the resazurin-based microliter dilution method [14]. Twofold serial dilutions of the extract (20–0.1 mg/mL) were prepared in Mueller–Hinton broth (MHB) and inoculated with bacterial suspensions (10^8 CFU/mL). After 24 h incubation at 37°C, 50 µL of resazurin solution (0.0015%) was added to each well, followed by incubation until color development. The MIC was recorded as the lowest extract concentration that prevented the color change from blue to pink, indicating inhibition of bacterial growth.

Anti-inflammatory Assay

The anti-inflammatory potential of the extract was evaluated through TNF-α protein expression (ELISA), COX-2 enzyme inhibition, and LOX inhibition assays as described below.

TNF-α protein expression (ELISA):

The experiment was performed as per kit instructions (GENLISATM Mouse TNF α ELISA- KB2145) 100 µl standard (TNF α - 1 µg/ml) and sample was added to the plate, plate was sealed and incubated for 2h at room temperature. The plate was washed four times with wash buffer (1X) and buffer was blotted by firmly tapping plate upside down on absorbent paper. Diluted detection antibody (Biotin Conjugated Detection Antibody) solution was added 100µl to each well, plate was sealed and incubated for an hour at room temperature. Again, plate was washed with wash buffer (1X) then 100µl diluted Streptavidin -HRP solution was added to each well, plate was sealed and incubated for an hour. Plate was washed with wash buffer (1X) and 100µl TMB substrate

(3,3',5,5'-Tetramethylbenzidine) solution was added and incubated in dark for 30 minutes. To stop the reaction, 100 µl of stop solution was added to each well and read the absorbance at 450nm within 30 minutes [15].

COX-2 Enzyme Inhibition Assay:

The in vitro inhibition of cyclooxygenase-2 (COX-2) activity was evaluated using a 96-well microplate assay [16]. Reaction mixtures contained Tris–Cl buffer (100 mM, pH 8.0), bovine hemin chloride (1 µM), and phenol (1 µM). The reaction was initiated by adding 5 µL of arachidonic acid (10 mM) as substrate and 5 µL of TMPD solution (17 mM), followed by incubation at room temperature for 10 min. Absorbance was measured at 595 nm using an ELISA microplate reader (iMark™, Bio-Rad). Celecoxib (2.5 mM) served as a positive control. IC_{50} values were calculated using GraphPad Prism version 6 (GraphPad Software, San Diego, CA, USA).

$$\text{Inhibition (\%)} = \frac{A_{Control} - A_{Test}}{A_{Control}} \text{x}100$$

where $A_{Control}$ = absorbance of the control and A_{Test} = absorbance of the sample.

Lipoxygenase (LOX) Inhibition Assay

Lipoxygenase (LOX) inhibition activity was assessed using a 96-well microplate assay [17]. Reaction mixtures contained LOX enzyme (500 U mL^{-1}; Sisco Research Laboratories, Cat. No. 9029-60-1) and Tris–HCl buffer (50 mM, pH 7.5). Samples were incubated at 37 °C for 15 min, followed by addition of 5 µL arachidonic acid substrate (2 mM). After 30 min at room temperature, 50 µL of FTC reagent (iron sulfate and ammonium thiocyanate) was added, and absorbance was measured at 490 nm using an ELISA microplate reader (iMark™, Bio-Rad). Quercetin (250 µg mL^{-1}) served as a positive control. IC_{50} values were determined using GraphPad Prism version 6 (GraphPad Software, San Diego, CA, USA).

$$\text{Inhibition (\%)} = \frac{A_{Control} - A_{Test}}{A_{Control}} \text{x}100$$

where $A_{Control}$ = absorbance of the control and A_{Test} = absorbance of the sample.

Drug Design and Drug-likeness:

The compounds identified via LC–MS analysis were subjected to drug-likeness prediction using the MolSoft computational platform (https://www.molsoft.com/), which evaluates molecular properties associated with oral bioavailability and drug-like behavior.

Molecular Docking:

The 3D structures of the target proteins were obtained from the PDB (https://www.rcsb.org/). The compound structures were retrieved from PubChem (https://pubchem.ncbi.nlm.nih.gov/). Docking was performed via AutoDock Vina and visualized with Discovery Studio [18].

Molecular dynamics (MD), principal component (PCA) and gmx_MMPBSA:

MD simulations (100 ns, 310 K) were used to assess the stability of the receptor–ligand complexes. The analyses included RMSD, RMSF, hydrogen bonding, and SASA. PCA was performed on the eigenvalues and visualized with XMGrace. Binding free energies were estimated via gmx_MMPBSA [18].

Quality Assurance and Control:

All the experiments were performed in triplicate. Analytical-grade solvents/reagents and standard protocols were used. The LC–MS instrument was calibrated. For the biological assays, positive controls (quercetin, amphotericin B, and celecoxib) were used. The cytotoxicity assays included untreated and blank wells. The data were analyzed

with GraphPad Prism 6, and the IC_{50} values are reported as the means ± SEMs. Only reproducible results were considered.

Results

LC–MS analysis

LC–MS analysis of the methanolic extract revealed multiple alkaloids, flavonoids, glycosides, and other secondary metabolites, each of which presented different retention times and hit scores, as shown in Fig. 2. A total of 21 compounds were identified (Suppl. Table 1), and their retention times varied from 1.42 to 33.70 minutes. The notable alkaloids identified include 7-hydroxymitragynine, (S,S)-(+)-tetrandrine, gardneramine, aconitine, lycorine-diacetate, and brucine. Various flavonoid glycosides, including vitexin, isosilybin A, orientin, and apigenin derivatives, have also been identified. Among these, lycorine-diacetate (RT 20.02 min) presented the highest hit score (0.8144), indicating a robust match with the reference library. Compounds such as (-)-podophyllotoxin, ginsenoside compound K, and chrysanthellin B were identified with notably high hit scores, reflecting their considerable presence in the extract. The variety of identified compounds underscores the intricate chemical makeup of the sample.

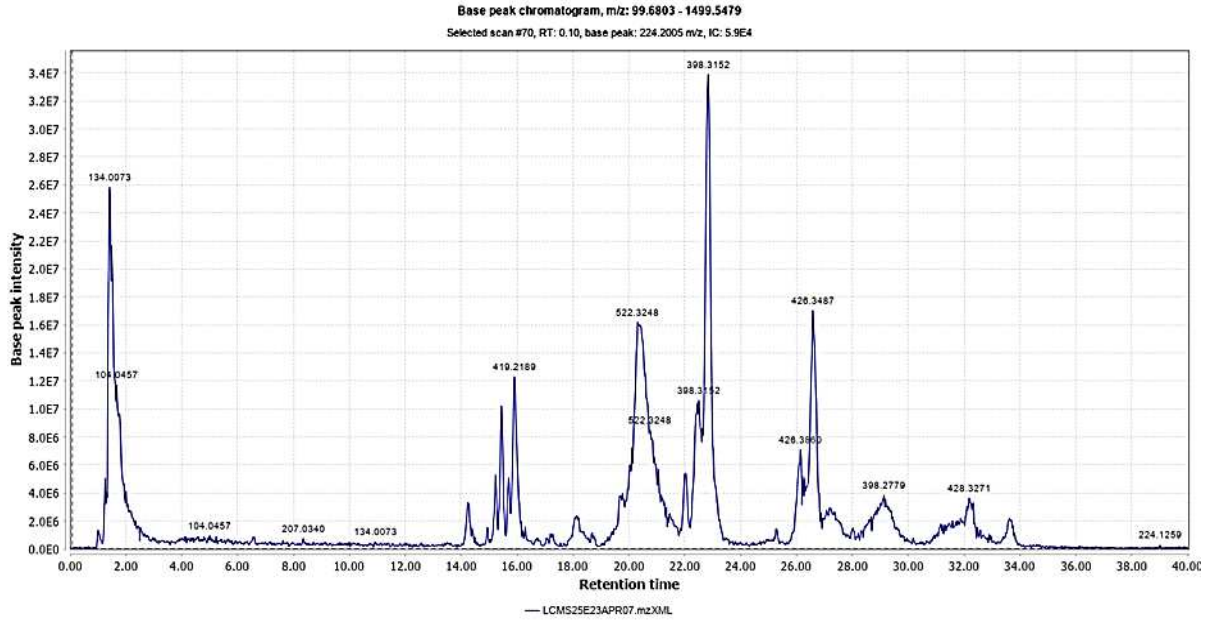

Fig. 2 LC–MS chromatogram of *S. mukorossi* extract showing peaks corresponding to identified compounds.

In vitro analysis

Cytotoxicity assessment (MTT assay)

The cytotoxicity of the plant extract was evaluated using the MTT assay in RAW 264.7 macrophage cells across a concentration range of 31.25–1000 µg/mL (Fig. 3). The extract exhibited low cytotoxicity, with cell viability exceeding 92% at 62.5 µg/mL, remaining above 85% at 250 µg/mL, and retaining approximately 71% viability at 1000 µg/mL. These results indicate that the extract is non-toxic to macrophages, even at its highest tested concentration. In contrast, treatment with the reference cytotoxic compound paclitaxel markedly reduced cell viability to below 50% at 100 µg/mL, confirming the assay's sensitivity and validating the biocompatibility of the plant extract. Microscopic examination revealed no detectable alterations in media color, cell morphology, or adhesion, further supporting the extract's safety profile [19].

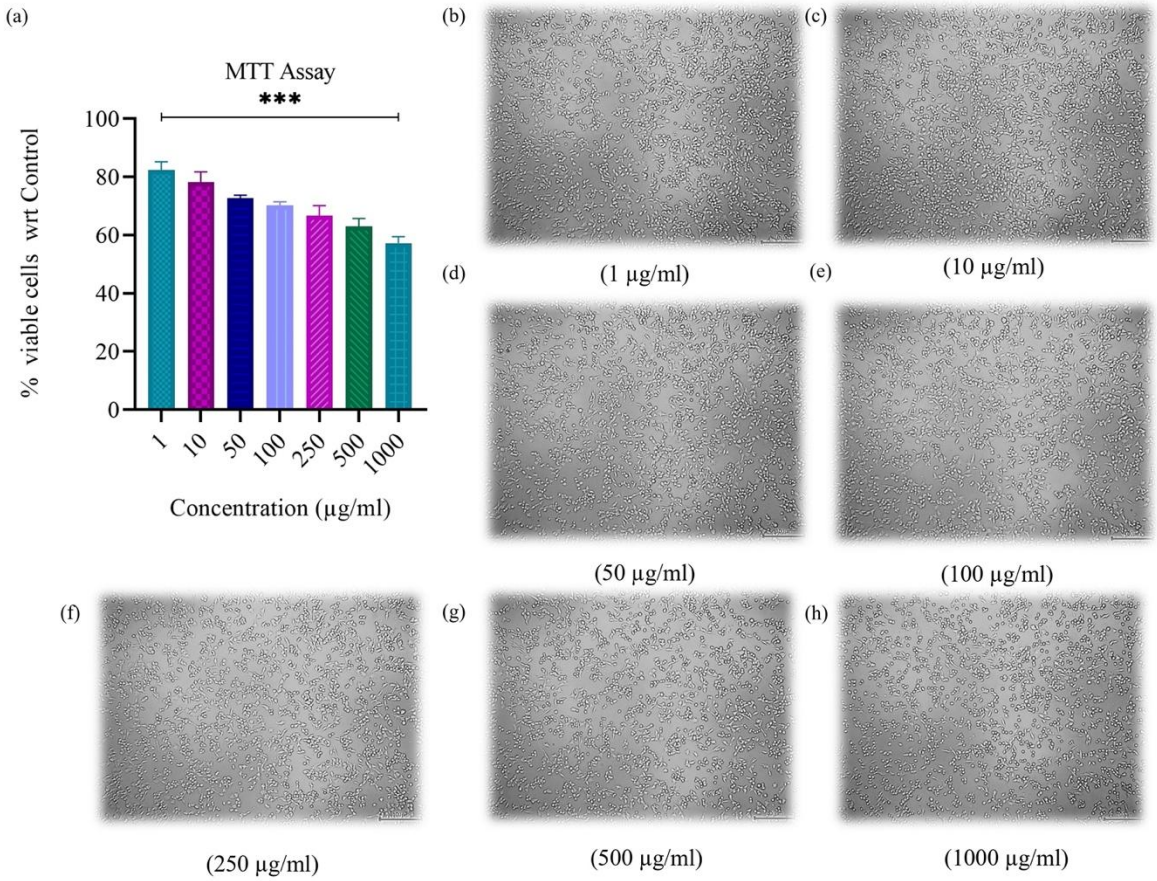

Fig. 3 MTT assay-based cytotoxicity evaluation of the effects of the plant extract on RAW 264.7 macrophages. **(a)** Percentage of viable cells relative to the control across different concentrations (1–1000 µg/ml) of the extract. **(b–h)** Phase-contrast microscopy images showing the cell morphology at various concentrations: (b) 1 µg/ml, (c) 10 µg/ml, (d) 50 µg/ml, (e) 100 µg/ml, (f) 250 µg/ml, (g) 500 µg/ml, and (h) 1000 µg/ml. The data revealed a significant decrease in cell viability with increasing concentrations (***$p < 0.001$).

Antimicrobial Assay

The antibacterial activity, evaluated by agar well diffusion, strongly inhibited *E. coli*, *S. aureus*, and *K. pneumoniae* (Fig. 4 a). MIC analysis revealed the strongest effect against *E. coli* (3.12 mg/ml), followed by *S. aureus* (6.25 mg/ml) and *K. pneumoniae* (12.5 mg/ml). These results confirm that *S. mukorossi* exhibits broad-spectrum antimicrobial activity, with *E. coli* being the most susceptible.

The antifungal activity of the *S. mukorossi* extract was assessed against *C. albicans* via the disc diffusion method. At 100 µg, the extract produced a 9 mm inhibition zone, whereas it was 7 mm for the control (70 µg), indicating significant antifungal potential (Fig. 4 b).

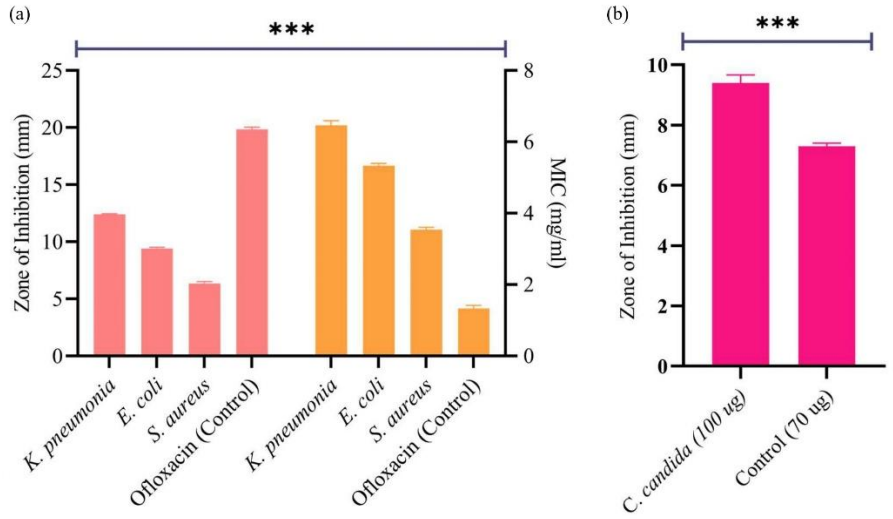

Fig. 4 (a) Determination of antimicrobial, MIC and (b) antifungal activities of the extract

TNF-α expression analysis (ELISA)

The influence of *S. mukorossi* seed extract on the production of the proinflammatory cytokine TNF-α was evaluated in RAW 264.7 macrophages using quantitative ELISA (Fig. 5a). Untreated control cells exhibited a basal TNF-α concentration of 3311.36 pg/mL, representing normal, non-inflammatory conditions. Stimulation with lipopolysaccharide (LPS) markedly increased TNF-α secretion by 24.09 pg/mL, confirming effective macrophage activation and induction of an inflammatory response. When macrophages were treated with the *S. mukorossi* extract alone, TNF-α levels increased only slightly (6.82 pg/mL), indicating negligible proinflammatory effects. However, co-treatment with LPS and the extract significantly reduced TNF-α secretion compared with the LPS-only group, with concentrations decreasing to 16.36 pg/mL and approximately 40.45 pg/mL at higher doses of the extract. These findings suggest that the *S. mukorossi* seed extract exerts a dose-dependent inhibitory effect on TNF-α production, demonstrating its potential anti-inflammatory activity [20].

Cyclooxygenase-2 (COX-2) Inhibition Assay

The inhibitory potential of the *S. mukorossi* seed extract against cyclooxygenase-2 (COX-2) was evaluated using a colorimetric assay based on the oxidation of N,N,N′,N′-tetramethyl-p-phenylenediamine (TMPD) at 595 nm (Fig. 5b). The extract demonstrated a concentration-dependent inhibition of COX-2 activity, exhibiting an IC_{50} value of 704.8 ± 0.02 µg/mL. In comparison, the standard COX-2 selective inhibitor celecoxib showed a markedly lower IC_{50} value of 682 ± 0.02 µM, confirming its higher pharmacological potency. Across the tested concentration range (31.25–1000 µg/mL), the *S. mukorossi* extract displayed a progressive increase in enzyme inhibition, rising from approximately 12% at 62.5 µg/mL to over 58% at 1000 µg/mL. This trend indicates a significant interaction of the extract with the COX-2 enzymatic pathway, particularly at higher concentrations [20].

Lipoxygenase (LOX) Inhibition Assay

The inhibitory activity of the *S. mukorossi* seed extract on the lipoxygenase (LOX) pathway was assessed using the ferric thiocyanate colorimetric assay (Fig. 5c). The extract demonstrated a concentration-dependent suppression of LOX activity, with an IC_{50} value of 598 µg/mL. Inhibition initiated at approximately 11.23% at 1 µg/mL and progressively increased to nearly 65% at 1000 µg/mL, indicating substantial attenuation of LOX enzymatic activity with increasing extract concentration. In comparison, quercetin, used as a reference LOX inhibitor, exhibited potent activity with an IC_{50} value of 21.59 µg/mL, rendering it approximately 28-fold more effective than the plant extract. The inhibition data were consistent across three independent replicates, and no

turbidity or chromogenic interference was observed during the assay, ensuring the reliability and precision of the photometric measurements [21].

Gene expression analysis – iNOS (conventional PCR)

Exposure to the effective concentration of *S. mukorossi* seed extract resulted in a significant alteration in iNOS gene expression in RAW 264.7 macrophages (Fig. 5d). In contrast to the untreated control group, which presented a normalized iNOS expression level of 0.50, the treated group (cell + plant sample) presented an increased expression of 1.10. This indicates a 2.2-fold increase in iNOS mRNA levels. Densitometric examination of the PCR bands validated the consistency of this increase across biological replicates, using GAPDH as the internal reference gene for normalization. The results demonstrated that the plant extract stimulated iNOS gene expression under the tested experimental conditions [22].

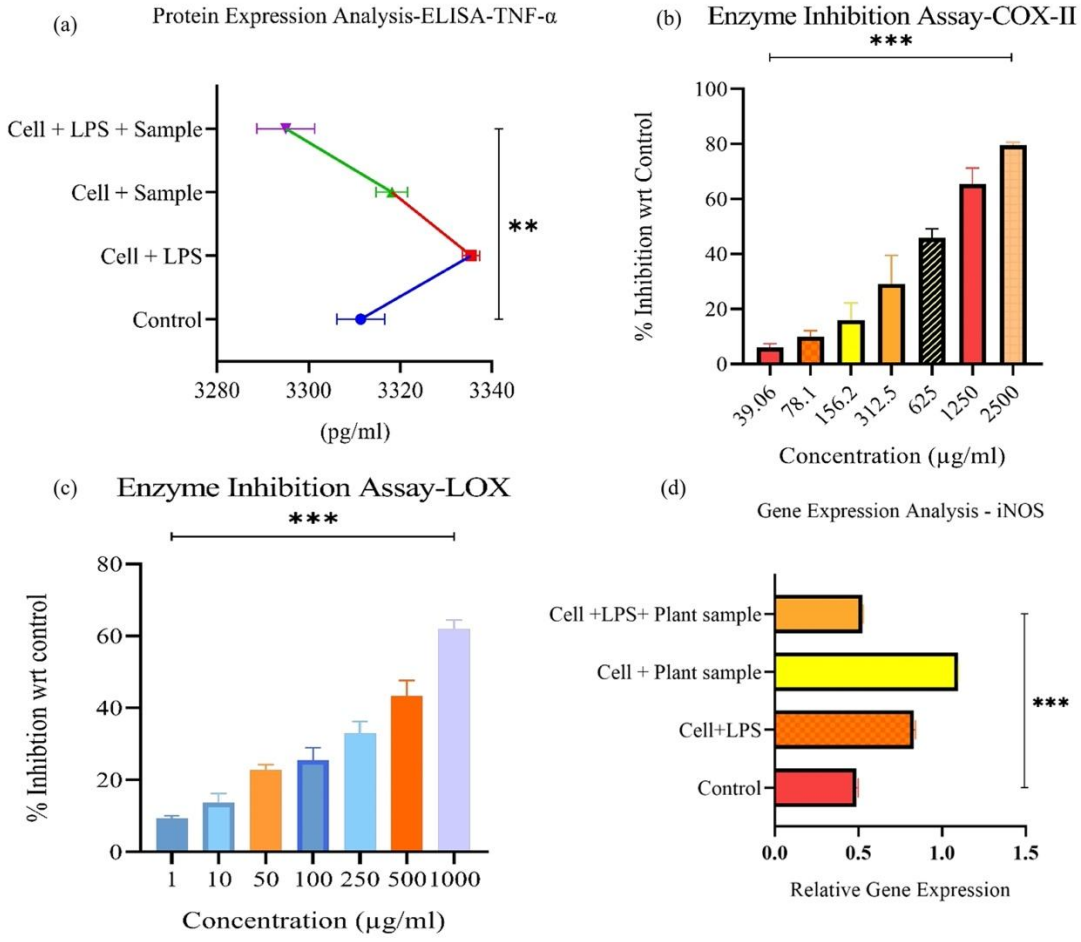

Fig. 5 In vitro anti-inflammatory activity of the plant extract. Figure (a) ELISA results showing reduced TNF-α levels in LPS-treated cells after extract treatment ($p < 0.01$). (b) COX-II inhibition increased with increasing extract concentration, peaking at 2500 µg/ml ($p < 0.001$). (c) LOX inhibition also increased in a dose-dependent manner, with the greatest increase occurring at 1000 µg/ml ($p < 0.001$), and (d) iNOS expression induced by LPS was suppressed by the extract ($p < 0.001$).

Drug-likeness

The drug-likeness and physicochemical properties of the selected ligands were evaluated to assess their potential as anti-hemorrhoidal compounds, as detailed in Table 2. The compounds oxyacanthine and (+)-tubocurarine chloride presented greater molecular weights (608.29 and 644.27 Da) and increased LogP values (5.16 and 5.43), suggesting possible difficulties in oral bioavailability. The topological polar surface area (MolPSA) varied among ligands, with Orientin (159.67 Å²) and Vitexin (144.19 Å²) exhibiting greater polarity, which may affect absorption and membrane permeability. BBB scores were predominantly low for the majority of ligands (<2),

indicating restricted central nervous system penetration. The number of stereocenters varied from 2--5, adding to the molecular complexity. The findings revealed that isosilybin A, vitexin, and orientin presented the most advantageous physicochemical features and drug likeness, making them attractive candidates for further development.

Table 2 Physicochemical Properties and Drug Likeness Parameters of Selected Compounds

Property	Vitexin	Isosilybin A	Oxyacanthine	(+)-Tubocurarine chloride	Orientin
Molecular formula	C21 H2O O10	C25 H22 O10	C37 H40 N2 O6	C37 H41 N2 O6.Cl	C21 H2O O11
Molecular weight	432.11	482.12	608.29 (>500)	644.27 (>500)	448.1
Number of HBA	10	10	8	7	11 (>10)
Number of HBD	7 (>5)	5	1	2	8 (>5)
MolLogP	0.77	1.91	5.16 (>5)	5.43 (>5)	0.33
MolLogS (Log(moles/L)/mg/L)	-0.00027	-0.0008	-0.41382	-1.83849	-0.00019
MolPSA (Å²)	144.19	126.94	59.34	63.13	159.67
MolVol (Å³)	391.88	439.51	632.45	642.11	404.61
pKa of most Basic/Acidic group	<0./6.42	<0./8.29	9.13/10.31	9.06/10.10	<0./6.42
BBB Score	1.7	1.21	2.94	2.8	1.66
Number of stereo centers	5	4	2	2	5
Drug-likeness model score	0.6	0.84	1.08	1.09	0.59

Molecular docking

Molecular docking research demonstrated that all the chosen ligands had advantageous binding affinities for IRAK4 (Table 3). Isosilybin A exhibited the most robust binding, as evidenced by a docking score of –10.6 kcal/mol, a ligand efficiency of 0.89, and the lowest inhibition constant of 12 nM, indicating significant promise as an IRAK4 inhibitor. Orientin (OE) and vitexin (VX) exhibited significant interactions, with binding affinities of –10.0 kcal/mol and –9.7 kcal/mol, respectively, albeit with marginally elevated Ki values of 53 nM and 66 nM. These findings identify isosilybin A as the most promising choice for targeting IRAK4, followed by orientin and vitexin. Importantly, since all the compounds displayed binding affinities below –5 kcal/mol, they can be considered to possess drug-like potential, supporting their prospective role as anti-hemorrhoidal agents.

Table 3 Binding affinity, ligand efficiency, and inhibition constants of selected compounds against IRAK4

Target	Ligand	Binding affinity (kcal/mol)	Ligand efficiency	Inhibit constant [d](KI) (nM)
IRAK4	Isosilybin A	-10.6	0.89	12
	Orientin	-10.0	0.82	53
	Vitexin	-9.7	0.87	66

MD simulation

The RMDS analysis of the protein–ligand complexes revealed consistent trajectories throughout the 100 ns simulation. The IRAK4–Isosilybin A (IRAK4-ISO) and IRAK4–Orientin (IRAK4-OE) complexes demonstrated stability, with RMSD fluctuations ranging from 0.2 to 0.25 nm, indicating minimal structural deviations (Fig. 6 a). In contrast, IRAK4–Vitexin (IRAK4-VX) presented increased RMSD values (~0.35–0.4 nm), suggesting a greater degree of conformational flexibility (Fig. 5a).

The RMSF plot identified regions exhibiting increased residue flexibility. IRAK4–VX displayed increased fluctuations in particular loop regions, whereas the IRAK4-ISO and IRAK4-OE complexes showed diminished residue-level mobility, suggesting more stable binding interactions (Figure 6b).

The SASA demonstrated consistent solvent exposure for IRAK4 across all complexes (Fig. 6c). The IRAK4-ISO and OE complexes presented slightly increased surface areas (~220–240 nm²), whereas the IRAK4-

VX complex presented a decreased solvent-accessible surface area (SASA) (~200–210 nm²), indicating denser packing or partial occlusion of residues during ligand interaction.

The hydrogen bonds varied across the complexes, as illustrated in Fig. 6d. IRAK4-ISO and OE maintained 1–3 stable hydrogen bonds throughout the simulation, thereby improving their binding stability. The VX complex demonstrated intermittent hydrogen bond formation, indicating weaker or transient interactions with IRAK4.

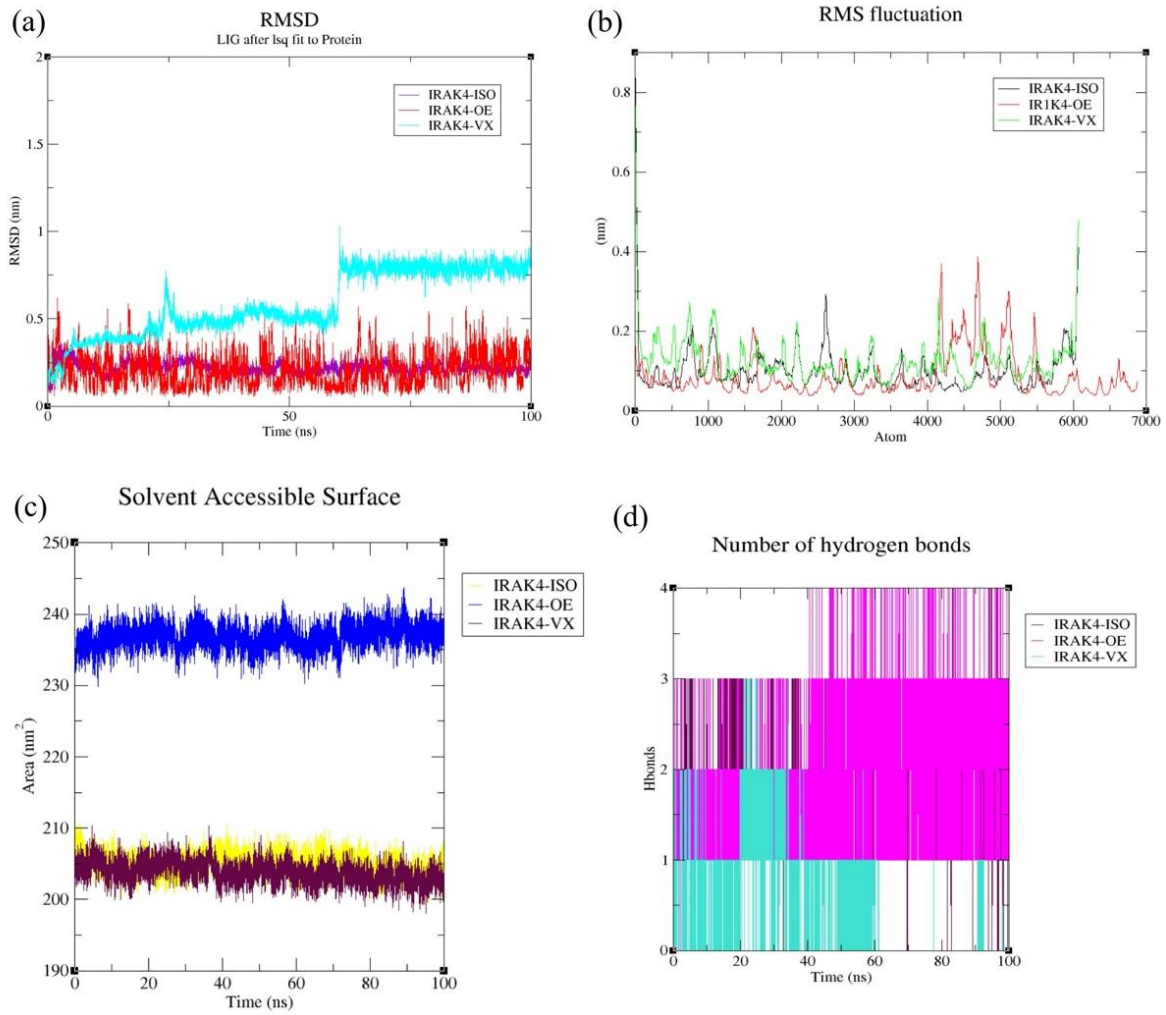

Fig. 6 Molecular dynamics simulation analyses of IRAK4–ligand complexes. (a) RMSD of the ligand after least-square fitting to the protein, (b) RMSF of the protein atoms, (c) SASA and (d) number of hydrogen bonds formed during the simulation.

PCA ANALYSIS

PCA, also known as essential dynamics (ED), was conducted to identify the predominant motions within the protein–ligand complexes. The trajectories were overlaid on Cα atoms to eliminate translational and rotational motions, and a covariance matrix was generated via gmx covar. The initial two principal components accounted for 45% (PC1) and 20% (PC2) of the variance. The 2D projection (Fig. 7) revealed distinct clustering: ISO formed a compact and stable cluster, OE sampled a broader conformational space indicative of flexibility, whereas VX displayed intermediate behavior with some overlap. These results demonstrate that ligand binding influences protein dynamics, resulting in different levels of stabilization among the complexes.

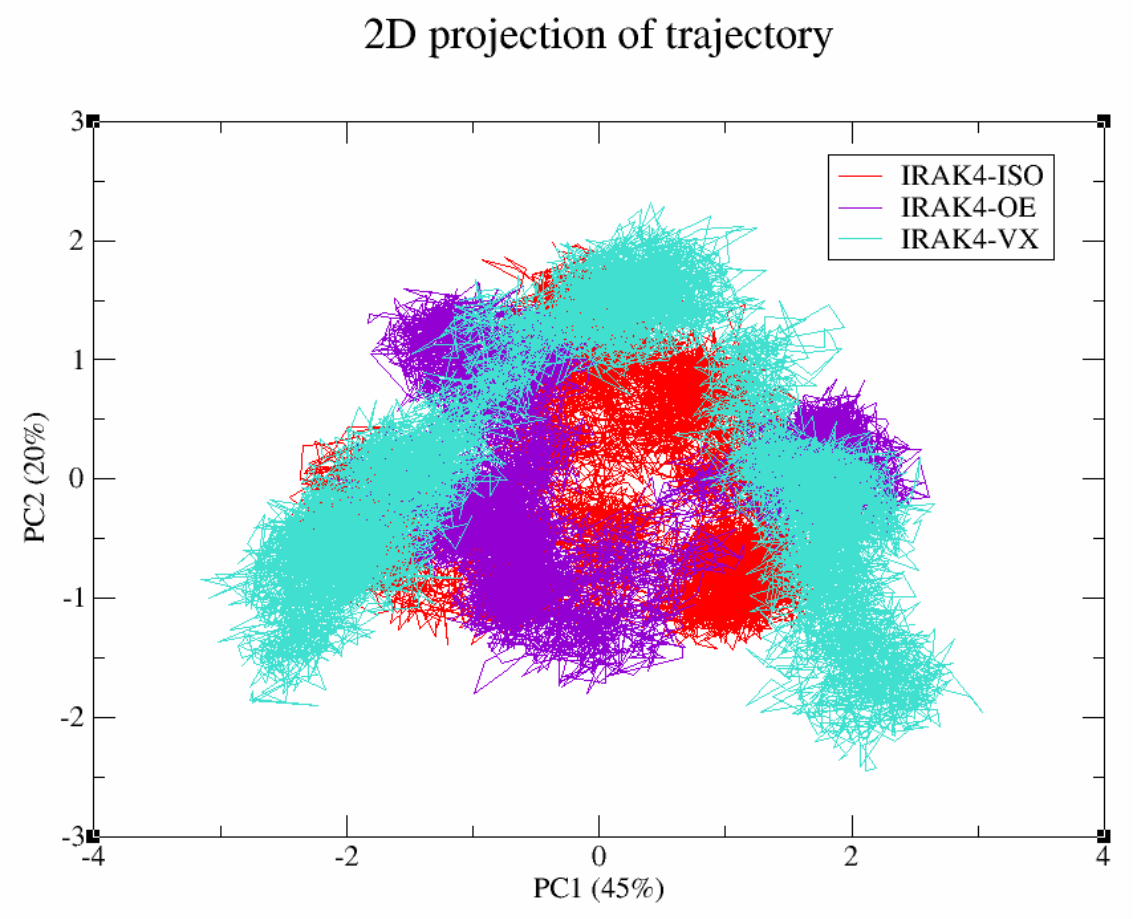

Fig. 7 PCA of the protein–ligand complexes. The 2D projection of trajectories along the first two principal components (PC1: 45%, PC2: 20%) is shown for the IRAK4-ISO, OE, and VX complexes. Distinct clustering patterns indicate the differential conformational sampling induced by ligand binding.

gmx_MMPBSA

The gmx_MMPBSA analysis provided detailed insights into the binding free energies of the three candidate compounds (ISO, OE, and VX) with the receptor (Table 4). ISO demonstrated the highest binding affinity, with a total free energy (ΔGbind) of -47.89 kcal/mol, predominantly driven by van der Waals interactions (ΔVDWAALS = -48.44 kcal/mol) and supported by moderate electrostatic contributions (ΔEEL = -8.58 kcal/mol). The solvation energy (ΔGSOLV = 9.13 kcal/mol) had a negligible influence on the interaction; however, the overall binding remained highly favorable. VX exhibited an intermediate ΔGbind of -27.69 kcal/mol. This value reflects stabilizing contributions from van der Waals interactions (ΔVDWAALS = -38.29 kcal/mol) and favorable solvation (ΔGSOLV = -31.41 kcal/mol), which are countered by a notably unfavorable electrostatic term (ΔEEL = +42.02 kcal/mol). The OE had the lowest binding affinity, with a ΔGbind of -19.25 kcal/mol. The positive electrostatic interaction (ΔEEL = -37.28 kcal/mol) was counterbalanced by considerable desolvation penalties (ΔEGB = 32.89 kcal/mol; ΔGSOLV = 30.52 kcal/mol) (Fig. 8).

Table 4 Binding free energy of protein–ligand complexes calculated via gmx_MMPBSA for anti-inflammatory activity.

Energy Component	ISO	OE	VX
ΔVDWAALS	-48.44	-12.49	-38.29
ΔEEL	-8.58	-37.28	42.02
ΔEGB	15.64	32.89	-26.34
ΔESURF	-6.51	-2.37	-5.08
ΔGGAS	-57.02	-49.77	3.73
ΔGSOLV	9.13	30.52	-31.41
ΔGbind	-47.89	-19.25	-27.69

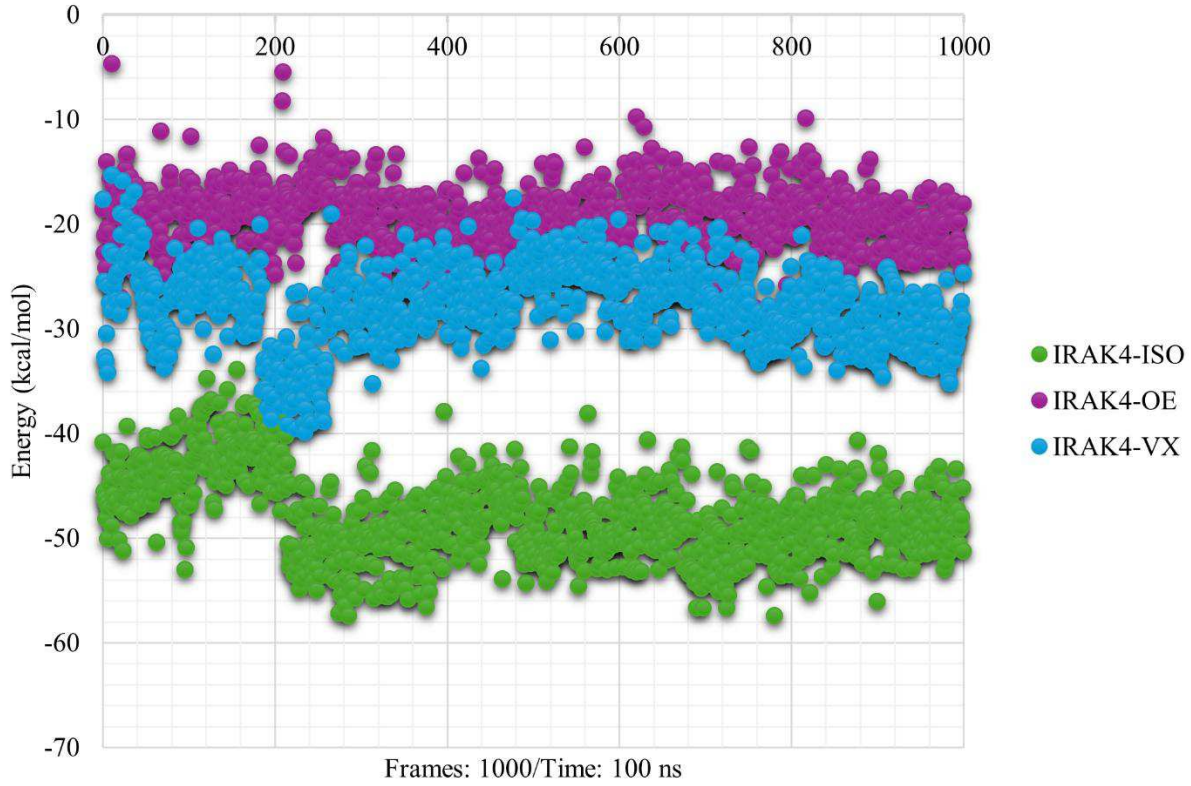

Fig. 8 Total binding free energy of protein–ligand complexes obtained from gmx_MMPBSA analysis for anti-inflammatory activity.

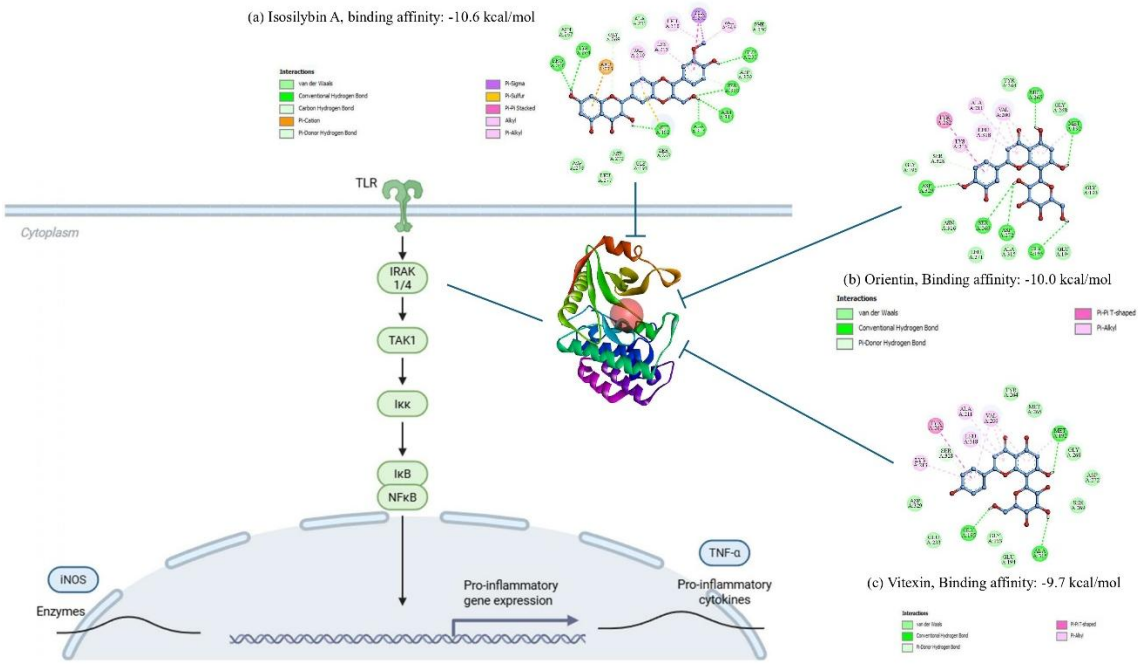

Fig. 9 In silico inhibition of IRAK4 within the TLR signaling pathway validated by downstream in vitro expression studies of TNF-α and iNOS, showing anti-inflammatory potential. Created with Biorender.

Discussion

LC–MS profiling of *Sapindus mukorossi* seed extract revealed a wide array of secondary metabolites, including alkaloids, flavonoids, saponins, and glycosides, highlighting its substantial pharmacological potential (Suppl. Table 1). The identification of alkaloids such as aconitine and brucine reflects the presence of compounds with strong bioactivities, but their known toxicity underscores the importance of dosage regulation and careful therapeutic evaluation. In contrast, flavonoids, including vitexin, orientin, and isosilybin A, are prominent compounds associated with long-term antioxidant, hepatoprotective, and anti-inflammatory properties. Additionally, the detection of podophyllotoxin, a well-established anticancer compound, and ginsenoside compound K, which is recognized for its adaptogenic effects, reflects the chemical diversity and broad pharmacological applications of the extract [23]. Among these metabolites, lycorine-diacetate was notable because of its elevated hit score, suggesting a potential key role in driving bioactivity. These findings collectively support the ethnomedicinal reputation of *S. mukorossi* seeds while simultaneously emphasizing the need for further isolation of active fractions and toxicological assessment [24].

Safety remains a major prerequisite in the development of botanical preparations, especially for chronic conditions such as hemorrhoids, where prolonged administration is anticipated. In this context, the MTT cytotoxicity assay demonstrated that the *S. mukorossi* extract was nontoxic to immune cells at all the tested concentrations, including the highest exposure dose, confirming its favorable safety profile [25]. This low cytotoxicity underscores its suitability for both typical and systemic formulations and highlights its compatibility with the immune system. Such biocompatibility is particularly valuable for patients seeking natural alternatives to conventional therapies such as corticosteroids or NSAIDs, which are often associated with adverse effects of long-term use.

The antimicrobial assays further revealed significant activities against pathogenic microorganisms relevant to hemorrhoidal disease. The extract inhibited *Candida albicans* with a 7 mm inhibition zone and was slightly less potent than amphotericin B (9 mm), thereby supporting its ethnopharmacological role in treating fungal infections. Although not a replacement for synthetic antifungals, this activity has potential for complementary use in resource-limited settings where access to standard drugs may be restricted. In addition, antibacterial assays confirmed the inhibitory effects against *E. coli, K. pneumoniae,* and *S. aureus,* key pathogens implicated in perianal infections. Interestingly, the higher MICs observed in *E. coli* than in *K. pneumoniae* and *S. aureus* align with known resistance profiles of these organisms in clinical practice [26]. The ability of the extract to act against antibiotic-resistant *E. coli* strains is particularly relevant, given the increasing global burden of antimicrobial resistance [27]. Mechanistically, the antimicrobial properties of *S. mukorossi* may involve multiple pathways, such as disruption of bacterial membranes, interference with nucleic acid synthesis, suppression of energy metabolism, and inhibition of biofilm formation [28, 29]. These diverse actions provide therapeutic advantages in preventing postoperative infections and promoting wound healing in hemorrhoidal management.

In addition to exhibiting antimicrobial efficacy, the *S. mukorossi* extract demonstrated notable anti-inflammatory and immunomodulatory properties. The level of TNF-α, a central proinflammatory cytokine involved in hemorrhoid pathology, was moderately reduced in LPS-stimulated macrophages treated with the extract, suggesting that its immunomodulatory potential may be mediated through the suppression of NF-κB signaling or IRAK4 inhibition [30]. Furthermore, the extract partially inhibited COX-2 activity, although with lower potency than did celecoxib, validating its ethnopharmacological application in alleviating pain, swelling, and vascular changes associated with hemorrhoids [31]. Similarly, the inhibition of LOX activity at higher concentrations, although weaker than that of the reference compound quercetin, suggests additional modulation of leukotriene-mediated inflammatory pathways [32]. Together, the inhibition of COX-2 and LOX reflects a multitarget pharmacological profile that is advantageous for treating multifactorial conditions such as hemorrhoids, where both prostaglandins and leukotrienes contribute to inflammation (Fig. 9). Interestingly, treatment also resulted in more than twofold upregulation of iNOS expression, suggesting that the extract plays a dual role—modestly suppressing inflammatory mediators while simultaneously enhancing nitric oxide-mediated macrophage activity, tissue repair, or microbial defense [33]. This finding emphasizes the importance of dose and cellular context in shaping the overall immune response. Collectively, the in vitro data demonstrate that *S. mukorossi* combines antimicrobial, anti-inflammatory, and immunomodulatory actions, positioning it as a promising adjunct for the management of hemorrhoidal disease.

These in silico investigations provided mechanistic insights into the anti-inflammatory activity observed in vitro, particularly implicating IRAK4 as a key molecular target. Drug-likeness assessment highlighted isosilybin A, vitexin, and orientin as promising candidates, with physicochemical properties largely within Lipinski's rule of five. Isosilybin A displayed the most balanced profile (MW 482.12 Da, 5 HBDs, 10 HBAs, LogP 1.91), indicating favorable oral bioavailability. Vitexin (MW 432.11 Da, 7 HBDs, 10 HBAs) and orientin (MW 448.1 Da, 8 HBDs, 10 HBAs) also demonstrated acceptable properties, although their relatively large polar surface areas and relatively high HBD counts may influence membrane permeability [6]. Nonetheless, their drug-

likeness scores (0.6–0.84) and low predicted blood–brain barrier penetration support their potential as peripherally selective agents suitable for hemorrhoidal therapy.

Molecular docking results further demonstrated that isosilybin A, vitexin, and orientin strongly bind to the active site of IRAK4, suggesting their potential as upstream inhibitors of the TLR/IL-1R signaling pathway [34]. ELISA-based validation confirmed that these compounds reduced TNF-α secretion, while iNOS expression assays revealed the suppression of proinflammatory signaling, which was consistent with IRAK4 inhibition. Molecular dynamics (MD) simulations provided further support, with the IRAK4–isosilybin A (ISO) and IRAK4–orientin (OE) complexes maintaining stable trajectories over 100 ns, with minimal RMSD variations (~0.2–0.25 nm), whereas the IRAK4–vitexin (VX) complex displayed greater fluctuations (~0.35–0.4 nm), reflecting weaker stability [35]. RMSF analysis confirmed reduced residue mobility for the ISO and OE complexes, indicating effective stabilization of the binding site, whereas VX induced greater fluctuations in loop regions [34]. SASA revealed slightly larger solvent-exposed areas for ISO and OE (~220–240 nm²) than for VX (~200–210 nm²), suggesting that stable complexes preserve favorable surface accessibility [37].

Hydrogen bonding analysis demonstrated that ISO and OE maintained 1–3 persistent hydrogen bonds, enhancing complex stability, whereas VX showed sporadic and transient interactions [38]. Essential dynamics and PCA further revealed that ISO formed compact, rigid conformations associated with stronger stabilization, whereas OE exhibited more flexible sampling and VX showed intermediate stabilization [39]. Energy decomposition studies have indicated that ISO stability is driven primarily by hydrophobic and van der Waals interactions, whereas OE suffers from solvation-driven destabilization, and VX exhibits destabilizing electrostatic contributions despite some favorable solvation terms [6, 40]. These differences highlight the structural complementarity of ISO with IRAK4 as a decisive factor for binding efficiency.

Taken together, these findings identify isosilybin A as the most promising lead compound, with orientin serving as a secondary candidate, for further optimization as a natural IRAK4 inhibitor. The mechanistic ability of these compounds to suppress IRAK4-mediated NF-κB activation and reduce the levels of proinflammatory mediators such as TNF-α and iNOS establishes a rational basis for their potential antihemorrhoidal application. The integration of LC–MS metabolite profiling, in vitro bioassays, and in silico modeling underscores the therapeutic relevance of *S. mukorossi* phytoconstituents and provides a foundation for future fractionation, isolation, and preclinical evaluation.

Conclusion

The methanolic extract of *Sapindus mukorossi* seed kernels has notable anti-inflammatory potential through the modulation of key inflammatory mediators, including TNF-α, COX-2, and LOX, and presents a favorable safety profile in immune cell models. The ability of the extract to increase iNOS expression indicates a multifaceted immunomodulatory function that could play a role in both resolving inflammation and facilitating tissue repair. Molecular docking and GMX molecular dynamics simulations revealed isosilybin A and orientin as effective inhibitors of IRAK4, a crucial kinase in inflammatory signaling pathways, thereby offering a molecular foundation for plant efficacy. The results provide scientific support for the traditional use of *S. mukorossi* in treating inflammatory conditions such as hemorrhoids and promote additional pharmaceutical research. Future studies should focus on isolating individual bioactive compounds, assessing their efficacy in vivo, and clarifying detailed molecular mechanisms to create innovative, multitarget anti-inflammatory agents. The incorporation of *S. mukorossi* derivatives into standardized natural formulations presents a promising avenue for developing effective and safer alternatives to traditional anti-inflammatory therapies.

Acknowledgment

The authors thank UGC for the National Fellowship for Higher Education for Schedule Tribe Students (NFST) for providing financial assistance during the research. The authors are also thankful to Dr. K. S. Devi, Department of Botany, Mizoram University, for helping in the identification of the plant sample.

Authors' contributions

E.L, H.S, L: Performed experiments, study design, data analyses and prepared original draft of manuscript. M.L, L and L.R: Critical review and editing of the manuscript. L.R: Supervised the study, contributed to drafting, revising and critically reviewing the manuscript.

Funding

The authors have no relevant financial or nonfinancial interests to disclose.

Data availability

The data will be made available upon request.

Author information

Ethics approval and consent to participate

Not applicable

Consent for publication

Not applicable

Competing interests

The authors declare no competing interests

References

1. Kornsteiner M, Wagner K, Elmadfa, I. Tocopherols and total phenolics in 10 different nuttypes. Food Chem. 2006; 98: 381–387. https://doi.org/10.1016/j.foodchem.2005.07.033
2. Shin T, Fujikawa K, Moe AZ, et al. Traditional knowledge of wild edible plants with special emphasis on medicinal uses in Southern Shan State, Myanmar. J. Ethnobiol. Ethnomed. 2018; *14*, 48. https://doi.org/10.1186/s13002-018-0248-1
3. Seal T. Determination of nutritive value, mineral contents and antioxidant activity of some wild edible plants from Meghalaya State, India. Asian J Appl Sci. 2011; 4:238–246. https://doi.org/10.3923/ajaps.2011.238.246
4. Indrayanto G. The importance of method validation in herbal drug research. J. Pharm. Biomed. Anal. 2022; 214, 114735. https://doi.org/10.1016/j.jpba.2022.114735
5. Atanasov AG, Zotchev SB, Dirsch VM, Orhan IE, Banach M, Rollinger JM, Barreca D, Weckwerth W, Bauer R, Bayer E, et al. Natural products in drug discovery: Advances and opportunities. Nat. Rev. Drug Discov. 2021; 20(3), 200–216. https://doi.org/10.1038/s41573-020-00114-z
6. Sailo H, Khiangte L, Lalremliani, Ralte L, Singh SP, Singh YT. Exploring the nutritional and antimicrobial properties of wild fruit, Castanopsis tribuloides: in vitro and in silico insights for potential antimicrobial drug development. Scientifica. 2025; 2106755. https://doi.org/10.1155/2025/2106755
7. Agidew MG. Phytochemical analysis of some selected traditional medicinal plants in Ethiopia. Bull Natl Res Cent. 2022; 46:87. https://doi.org/10.1186/s42269-022-00793-4
8. Selvaraj A, Valliammai A, Premika M, Priya A, Bhaskar JP, Pandian SK. *Sapindus mukorossi* Gaertn. and its bioactive metabolite oleic acid impedes methicillin-resistant *Staphylococcus aureus* biofilm formation. Microbiol Res. 2021; 242:126601. https://doi.org/10.1016/j.micres.2020.126601
9. Chen CC, Nien CJ, Chen LG, Huang KY, Chang WJ, Huang HM. Effects of *Sapindus mukorossi* seed oil on skin wound healing: In vivo and in vitro testing. Int J Mol Sci. 2019; 20:2579. https://doi.org/10.3390/ijms20102579
10. Takagi K, Park EH, Kato H. Anti-inflammatory activities of hederagenin and crude saponin isolated from *Sapindus mukorossi*. Chem Pharm Bull. 2020; 68:1183–1188. https://doi.org/10.1248/cpb.cpb68.1183
11. Lalruatpuii E, Ngurtinkhuma RK, Lalruatfela S, Reddy KV. Usage and preservation of Mizo traditional medicine by the people of Chungtlang Village, Mamit District, Mizoram. J. Med. Libr. Assoc. 2024; 112(3), 286–292. https://doi.org/10.5195/jmla.2024.1765
12. Akhtar N, Wani AK, Mir TU, Kumar N, Mannan MA. *Sapindus mukorossi* : Ethnomedicinal uses, phytochemistry, and pharmacological activities. Plant Cell Biotechnol Mol Biol. 2021; 22:300–319
13. Oniszczuk A, Olech M, Oniszczuk T, Wojtunik-Kulesza K, Wójtowicz A. Extraction methods, LC–ESI–MS/MS analysis of phenolic compounds and anti-radical properties of functional food enriched with elderberry flowers or fruits. Arab J Chem. 2019; 12:4719–4730. https://doi.org/10.1016/j.arabjc.2015.07.018
14. Wiegand I, Hilpert K, Hancock RE. Agar and broth dilution methods to determine the minimal inhibitory concentration (MIC) of antimicrobial substances. Nat Protoc. 2008; 3:163–175. https://doi.org/10.1038/nprot.2007.521
15. Assas BM, Levison SE, Little M, England H, Battrick L, Bagnall J, Pennock JL. Anti-inflammatory effects of infliximab in mice are independent of tumor necrosis factor α neutralization. Clin Exp Immunol. 2017; 187:225–233. https://doi.org/10.1111/cei.12887
16. Cao H, Yu R, Choi Y, Ma ZZ, Zhang H, Xiang W, Lee DY, Berman BM, Moudgil KD, Fong HH, van Breemen RB. Discovery of cyclooxygenase inhibitors from medicinal plants used to treat inflammation. Pharmacol Res. 2010; 61:519–524. https://doi.org/10.1016/j.phrs.2010.02.007

17. Sharanya CS, Abhithaj J, Arun KG, Eeda KR, Bhat V, Variyar EJ, Sabu A, Haridas M. Lipoxygenase inhibitory synthetic derivatives of methyl gallate regulate gene expressions of COX-2 and cytokines to reduce animal model arthritis. Sci Rep. 2023; 13:10644. https://doi.org/10.1038/s41598-023-37613-z
18. Gogoi B, Chowdhury P, Goswami N, Gogoi N, Naiya T, Chetia P, Handique PJ. Identification of potential plant-based inhibitor against viral proteases of SARS-CoV-2 through molecular docking, MM-PBSA binding energy calculations and molecular dynamics simulation. Mol Divers. 2021; 25:1963–1977. https://doi.org/10.1007/s11030-021-10201-x
19. Kumar A, Rai Y, Bhatt AN. Anticancer drug-mediated increase in mitochondrial mass limits the application of metabolic viability-based MTT assay in cytotoxicity screening. Cytotechnology. 2024; 76:301–311. https://doi.org/10.1007/s10616-024-00690-5
20. Shah, M., Parveen, Z., & Khan, M. R. Evaluation of antioxidant, anti-inflammatory, analgesic and antipyretic activities of the stem bark of Sapindus mukorossi. BMC Complement. 2017; Altern. Med., 17(1), 526. https://doi.org/10.1186/s12906-017-2042-3
21. Sirisha, G. V. D., Rachel, K. V., Zaveri, K., Yarla, N. S., Kiranmayi, P., Ganash, M., Alkreathy, H. M., Rajeh, N., & Ashraf, G. M. Molecular docking and in vitro studies of soap nut trypsin inhibitor (SNTI) against phospholipase A_2 isoforms in therapeutic intervention of inflammatory diseases. Int. J. Biol. Macromol. 2018; 114, 556–564. https://doi.org/10.1016/j.ijbiomac.2018.03.139
22. Bomfim FRC, Gomes BS, Lanza SZ, Esquisatto MAM, Lopes-Filho GDJ. Photobiomodulation effects on synovial morphology, iNOS gene, and protein expression in a model of acute inflammation. Acta Cir Bras. 2024; 39:e392024. https://doi.org/10.1590/acb392024
23. Teoh WY, Yong YS, Razali FN, Stephenie S, Dawood Shah M, Tan JK, Mohd Esa N. LC–MS/MS and GC–MS analysis for the identification of bioactive metabolites responsible for the antioxidant and antibacterial activities of *Lygodium microphyllum* (Cav.) R. Br. Separations. 2023; 10:215. https://doi.org/10.3390/separations10030215
24. Zhang W, Jiang H, Yang J, Jin M, Du Y, Sun Q, Xu H. Safety assessment and antioxidant evaluation of betulin by LC–MS combined with free radical assays. Anal Biochem. 2019; 587:113460. https://doi.org/10.1016/j.ab.2019.113460
25. Chaudhry G, Zeenia, Safdar N, Begum S, Akim AM, Sung YY, Muhammad TS. Cytotoxicity assays for cancer drug screening: methodological insights and considerations for reliable assessment in drug discovery. Braz J Biol. 2024; 84:e284409. https://doi.org/10.1590/1519-6984.284409
26. Liang Y, Ren T, Li R, Yu Z, Wang Y, Zhang X, Luo C. Natural products with potential effects on hemorrhoids: a review. Molecules. 2024; 29:2673. https://doi.org/10.3390/molecules29112673
27. Liu CK, Liu CP, Leung CH, Sun FJ. Clinical and microbiological analysis of adult perianal abscess. J Microbiol Immunol Infect. 2011; 44:204–208. https://doi.org/10.1016/j.jmii.2011.01.024
28. Xie Y, Yang W, Tang F, Chen X, Ren L. Antibacterial activities of flavonoids: structure-activity relationship and mechanism. Curr Med Chem. 2015; 22:132–149. https://doi.org/10.2174/0929867321666140916113443
29. Yun DG, Lee DG. Antibacterial activity of curcumin via apoptosis-like response in *Escherichia coli*. Appl Microbiol Biotechnol. 2016; 100:5505–5514. https://doi.org/10.1007/s00253-016-7531-0
30. Otto G. IRAK4 inhibitor attenuates inflammation. Nat Rev Rheumatol. 2021; 17:646. https://doi.org/10.1038/s41584-021-00699-8
31. Haque MF, El-Nashar HA, Akbor MS, Alfaifi M, Bappi MH, Chowdhury AK, Islam MT. Anti-inflammatory activity of d-pinitol possibly through inhibiting COX-2 enzyme: in vivo and in silico studies. Front Chem. 2024; 12:1366844. https://doi.org/10.3389/fchem.2024.1366844
32. Mukhopadhyay N, Shukla A, Makhal PN, Kaki VR. Natural product-driven dual COX-LOX inhibitors: Overview of recent studies on the development of novel anti-inflammatory agents. Heliyon. 2023; 9:3. https://doi.org/10.1016/j.heliyon.2023.e13701
33. Wu KKL, Xu X, Wu M, Li X, Hoque M, Li GHY, Cheng KKY. MDM2 induces pro-inflammatory and glycolytic responses in M1 macrophages by integrating iNOS-nitric oxide and HIF-1α pathways in mice. Nat Commun. 2024; 15:8624. https://doi.org/10.1038/s41467-024-08624-7
34. Saleh HA, Yousef MH, Abdelnaser A. The anti-inflammatory properties of phytochemicals and their effects on epigenetic mechanisms involved in TLR4/NF-κB-mediated inflammation. Front Immunol. 2021; 12:606069. https://doi.org/10.3389/fimmu.2021.606069
35. Khiangte L, Sailo H, Ralte L, Lalnunmawia F, Senthilkumar N, Singh YT. In vitro and in silico evaluation of phytocompounds from Leucaena leucocephala and Entada phaseoloides targeting DNA gyrase, topoisomerase II, AKT1. Sci Rep. 2025; 15:25399. https://doi.org/10.1038/s41598-025-25399-7
36. Nghakliana F, Tochhawng L, Sailo H, Lalawmpuii R, Lalsangpuii F, Iyer M, Siama Z. In vitro evaluation of anticancer and apoptotic activity of Elaeagnus caudata Schltdl. with computational identification of a novel HSP90 inhibitor. Chem Biodivers. 2025; e00679. https://doi.org/10.1002/cbdv.202500679

37. Lalmuansangi C, Lalfakawmi, Nghakliana F, Sailo H, Tochhawng L, Trivedi AK, Siama Z. Anticancer activity of Stemona tuberosa (wild asparagus) against type-II human lung adenocarcinoma (A549) cells and identification of SRC inhibitor using integrated network pharmacology and molecular dynamic simulation. Discover Oncol. 2025; 16:429. https://doi.org/10.1007/s12672-025-00821-3
38. Ralte L, Sailo H, Kumar NS, Singh YT. Exploring the pharmacological potential of Lepionurus sylvestris Blume: from folklore medicinal usage to modern drug development strategies using in vitro and in silico analyses. BMC Complement Med Ther. 2024; 24:289. https://doi.org/10.1186/s12906-024-07268-9
39. Srikumar PS, Rohini K, Rajesh PK. Molecular dynamics simulations and principal component analysis on human laforin mutation W32G and W32G/K87A. Protein J. 2014; 33:289–295. https://doi.org/10.1007/s10930-014-9551-0
40. Elfiky AA, Mansour KR, Mohamed Y, Abdelaziz YK, Nicholls IA. Exploring the anticancer potential of proton pump inhibitors by targeting GRP78 and V-ATPase: molecular docking, molecular dynamics, PCA, and MM-GBSA calculations. Int J Mol Sci. 2025; 26:8170. https://doi.org/10.3390/ijms26178170

Supplementary Files

This is a list of supplementary files associated with this preprint. Click to download.

- suppl..docx